Chemical Physics Letters 603 (2014) 46–50

Contents lists available at ScienceDirect

Chemical Physics Letters

journal homepage: www.elsevier.com/locate/cplett

Site-specific formation of metastable dications following inner-shell ionization of CO_2

Y. Hikosaka [a,*], Y. Shibata [a], K. Soejima [a], H. Iwayama [b], E. Shigemasa [b]

[a] Department of Environmental Science, Niigata University, Niigata 950-2181, Japan
[b] UVSOR Facility, Institute for Molecular Science, Okazaki 444-8585, Japan

ARTICLE INFO

Article history:
Received 20 March 2014
In final form 17 April 2014
Available online 24 April 2014

ABSTRACT

An Auger-electron–ion coincidence method is applied to study the site-specific formation of metastable CO_2^{2+} in the C1s and O1s Auger decays of CO_2. It is found that only dication states with the electronic configuration of $1\pi_g^{-2}$ are relevant to the metastable formation. These dication states are favorably produced in the O1s Auger decay, because of the charge distribution of the $1\pi_g$ orbital localizing at the O site. Fragmentation channels of dissociative CO_2^{2+} states are also investigated.

© 2014 Elsevier B.V. All rights reserved.

1. Introduction

Inner-shell excitation/ionization in a molecule composed of light atoms is usually followed by Auger decay, which dominantly produces the molecular ion with holes in the valence shell. The core hole generated by the initial inner-shell excitation/ionization is localized at an atomic site, and then the localization should be to some extent preserved in the Auger final states. This view has led to the idea of site-specific fragmentation [1], or selective bond breaking around the specific atomic site where the initial core–hole is created. Site-specific fragmentation has been widely observed not only in gas-phase molecules [2,3] but also in adsorbed or condensed molecules [4].

The ion yield spectra in the C1s and O1s inner-shell ranges of CO_2 [5] show that the increase of the metastable CO_2^{2+} yield is more remarkable above the O1s threshold than above the C1s threshold. This observation indicates a unique site-specific phenomenon that metastable dication formation, not fragmentation, presents site-specificity. The site-specificity in the metastable dication formation is confirmed by the present investigation. Figure 1 shows time-of-flight spectra of ions observed in coincidence with C1s or O1s photoelectrons, which were obtained with the electron–ion coincidence spectrometer described in Section 2. While the difference in the intensities of each fragment ion is at most 40% between the two spectra, the metastable CO_2^{2+} yields associated with the O1s ionization are about three times larger than those with the C1s ionization.

In this Letter, we have studied the mechanism of the site-specific formation of metastable CO_2^{2+} following inner-shell ionization of CO_2, by using an Auger-electron–ion coincidence method. We have identified Auger final states associated with the formation of metastable CO_2^{2+}, as well as those with individual fragmentation channels. Only CO_2^{2+} states with two holes at the $1\pi_g$ orbital, which is the highest-occupied valence orbital in the neutral ground CO_2, are observed as metastable dications. These dication states are favorably formed by the O1s Auger decay, because of the large charge distribution of the $1\pi_g$ orbital at the O site.

2. Experimental

The experiment was performed at the undulator beamline BL6U in UVSOR. The synchrotron radiation was monochromatized by a grazing incidence monochromator using a varied-line-spacing plane grating. The detailed description of the electron–ion coincidence spectrometer used in the present work was already given elsewhere [6,7]. Briefly, the coincidence spectrometer consists of a double toroidal electron analyzer and a three-dimensional ion momentum spectrometer, each of which is equipped with a time- and position-sensitive delay line detector (Roentdek DLD40). It is worth mentioning that dissociation of singly-charged CO_2 ion states produced by resonant Auger decay of C1s excited states in CO_2 has been already investigated by the same kind of method as in the present study [8].

Electrons ejected at ~54.7° with respect to the electric vector of the incident light were sampled (the acceptance solid angle is 5% of 4π sr) and then were dispersed in energy by toroidal deflectors. Through the present measurements, the pass energy of the analyzer was set to 200 eV, and electrons within an energy range corresponding to 15% of the pass energy were observed simultaneously. The electron transmission efficiency as a function of electron kinetic energy was determined by observing Ar 3p

* Corresponding author. Fax: +81 25 262 6147.
E-mail address: hikosaka@env.sc.niigata-u.ac.jp (Y. Hikosaka).

http://dx.doi.org/10.1016/j.cplett.2014.04.030
0009-2614/© 2014 Elsevier B.V. All rights reserved.

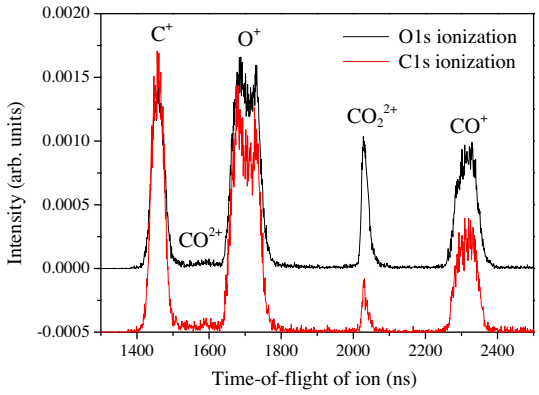

Figure 1. Time-of-flight spectra of ions observed in coincidence with C1s and O1s photoelectrons, which were observed at the photon energies of 403 eV and 643 eV, respectively. Intensities are normalized to the photoelectron counts. Signals in the time-of-flight range below 1400 ns were masked, to veto large noises resulting from the pulsed electric field for the ion extraction; the C^{2+} and O^{2+} peaks could not be observed accordingly.

photoelectron peaks at different photon energies. It was estimated that the electron energy resolution with the pass energy of 200 eV was around 3 eV (FWHM).

According to each electron detection, a pulsed electric field of 270 V/cm was applied to the interaction region, in order to extract the associated ions to the ion momentum spectrometer. The pulsed electric field ensured a 4π collection solid angle for ions with kinetic energies of less than 7 eV. In Figure 1, the O^+ peaks exhibit hollow shapes, which is probably due to escapes of higher kinetic energy ions whose emission directions are perpendicular to the flight tube. The ion observation allows multi-hit detection, which enables us to identify fragmentation channels from Auger final states. The detection efficiency of the ion detector was estimated to be ~43% by comparing coincidence yields for ion-pair $CO^+ + O^+$ and that for single-hit CO^+, both of which are produced from Auger final CO_2^{2+}. Contributions from false coincidences were evaluated to be negligible in the present measurements, by a separate coincidence measurement where the pulsed electric field for observing ions was triggered independent of electron detection.

Auger-electron–ion coincidence datasets were accumulated for CO_2 at photon energies of 403 eV (for C1s Auger decay) and 643 eV (for O1s Auger decay). At each photon energy, coincidence datasets were obtained with three different settings to kinetic energy window: one for observing inner-shell photoelectrons and the other two to cover the whole Auger spectral ranges.

3. Results and discussion

Figures 2a and 3a show C1s and O1s Auger spectra of CO_2, respectively, which were obtained from the total events in the coincidence datasets. Each spectrum was made by combining the spectra with two different kinetic-energy windows. These Auger spectra exhibit several band structures corresponding to the formation of different CO_2^{2+} states. The spectral features essentially agree with the previous measurements [9–11], though the vibrational structures of low-lying CO_2^{2+} states [11] cannot be resolved with the present resolution. In these figures, the same labels as in [9,12] are adopted to the band structures, and the assignments of the electronic configurations of these bands are presented in Table I of [12]. Some of the band structures are common in the two spectra, but the relative intensities are largely different between them. The lowest band (B1) around a binding energy of 38 eV is assigned to the formation of CO_2^{2+} states with two holes at the $1\pi_g$ orbital [12]. Different combinations of two valence holes

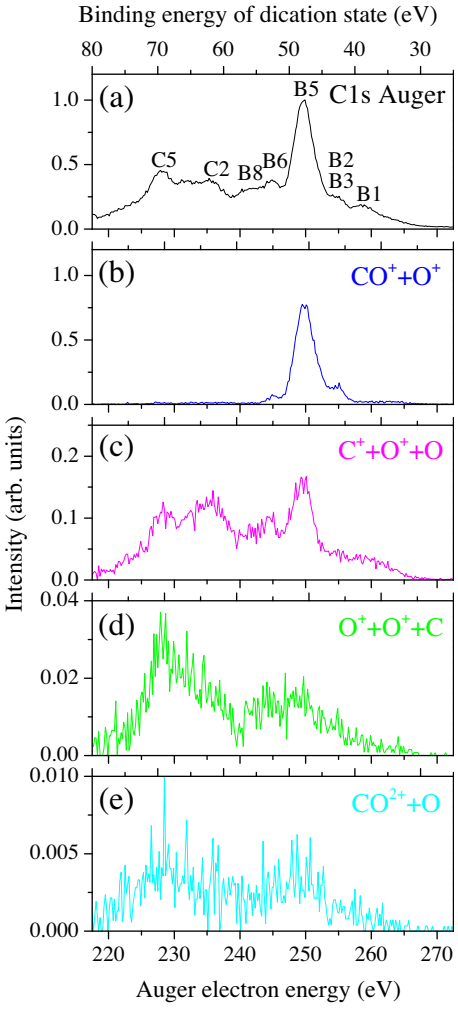

Figure 2. (a) C1s Auger spectrum of CO_2 derived from total events, and those filtered by coincidences with (b) $CO^+ + O^+$, (c) $C^+ + O^+$, (d) $O^+ + O^+$ and (e) CO^{2+}. The intensities of the coincidence Auger spectra are corrected by assuming the 43% detection efficiency for each single ion. The intensity of the $O^+ + O^+$ spectrum is underestimated, because of the detection dead time. The labels of the band structures, indicated in (a), are adopted from [9,12], and the assignments of their electronic configurations are presented in Table I of [12].

in the four outer-valence orbitals lead the band structures in the binding energy of 40–65 eV [12]. Peaks above 65 eV are attributed to states with a hole in the inner-valence orbitals [12]. Above the triple ionization threshold at 74 eV [13], a small contribution from double Auger decay forming triply-charged CO_2 ion should be included in the Auger yields. Note that the valence electronic configuration of the neutral ground state in CO_2 is $(3\sigma_g)^2(2\sigma_u)^2(4\sigma_g)^2(3\sigma_u)^2(1\pi_u)^4(1\pi_g)^4$, where the $3\sigma_g$ and $2\sigma_u$ orbitals are categorized to inner-valence orbital [14].

Prior to the investigation of metastable CO_2^{2+} formation, we pay attention to the dissociation channels of the CO_2^{2+} states. When the two positive charges of Auger final CO_2^{2+} states are localized in one of the fragments, the dissociation channel is observed as the coincidence between an Auger electron and a single dication fragment. Figure 4a shows a time-of-flight spectrum of single ions detected in coincidence with Auger electrons, which were extracted from the coincidence dataset accumulated for the C1s Auger decay with the kinetic energy window of 245–275 eV. Although possible dication fragments are C^{2+}, O^{2+}, CO^{2+} and O_2^{2+}, only a faint structure attributable to CO^{2+} is discernible in the time-of-flight spectrum. The O_2^{2+} fragments cannot be identified due to the overlap with

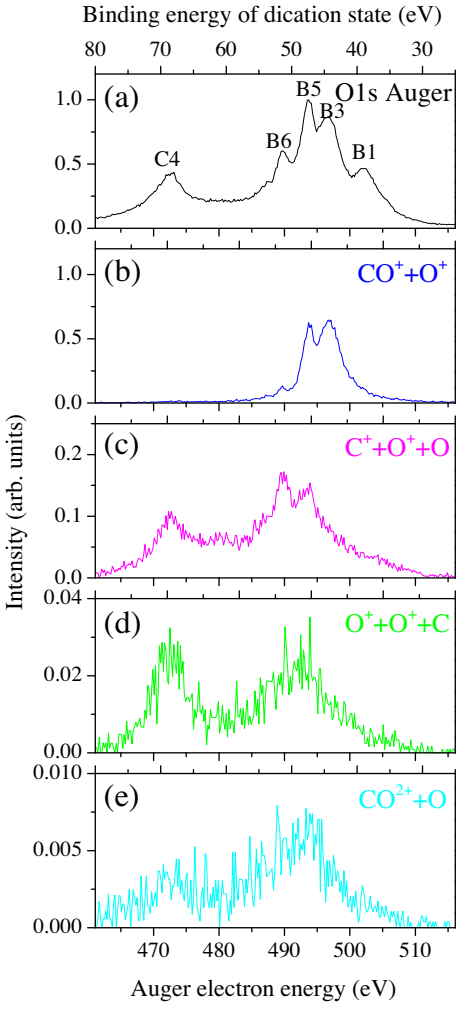

Figure 3. Same as Figure 2, for the O1s Auger decay of CO_2.

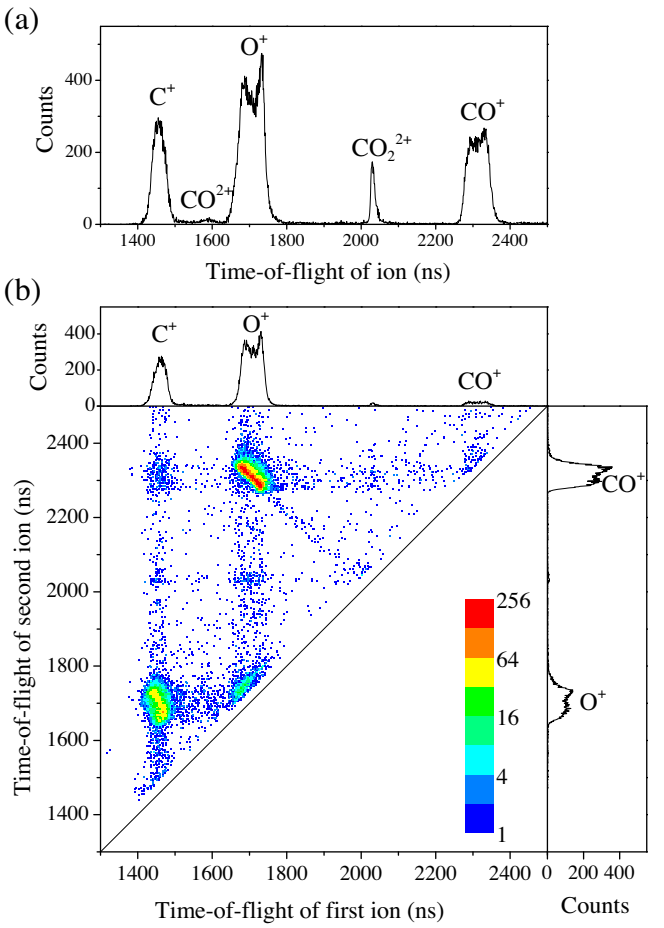

Figure 4. (a) Time-of-flight spectrum of single ions detected in coincidence with Auger electrons, and (b) two-dimensional map for times-of-flight of ion-pairs measured in coincidence with Auger electrons. They were derived from the coincidence dataset obtained for the C1s Auger decay with the kinetic energy window of 245–275 eV which corresponds roughly to the right-half range of the Auger spectrum in Figure 2a. The C^+, O^+ and CO^+ peaks in the time-of-flight spectrum in (a) result from ion pair events in which one of the ions are missed in the detection. On the map in (b), coincidence counts are plotted as a function of both time-of-flight of first ion (horizontal axis) and that of second ion (vertical axis), and are presented on a logarithmic scale. The time-of-flight spectra of the first and second ions, which are the projections of the coincidence counts on the map onto the horizontal and the vertical axes, are shown in the top and right panels, respectively.

the O^+ peak. The atomic dication fragments of C^{2+} and O^{2+} could not be observed in the present measurement, because the signals in the time-of-flight range below 1400 ns were masked in order to veto large noises resulting from the pulsed electric field for the ion extraction. Note that the C^+, O^+ and CO^+ peaks in the time-of-flight spectrum result from ion pair events in which one of the ions are missed in the detection.

Meanwhile, the dissociation channels forming fragment ion pairs should be identified as coincidences between an Auger electron and two fragment ions. Figure 4b shows a two-dimensional map for the correlations between two ions detected in coincidence with an Auger electron, extracted from the same coincidence dataset as for Figure 4a. On the two-dimensional map, clear structures for coincidences between fragment ion pairs of $CO^+ + O^+$, $C^+ + O^+$ and $O^+ + O^+$ can be identified, while any reasonable structure for the remaining pair of $O_2^+ + C^+$, whose formation needs a large conformation change, is indiscernible. The $CO^+ + O^+$ structure on this map shows a clear ridge with gradient of -1. This feature is characteristic of the coincidences between the two fragment ions from two-body dissociation in which the fragments are emitted into the opposite direction with an equal momentum. A weak diagonal tail can be found at the lower right-hand side of the $CO^+ + O^+$ structure, which continues to $(x, y) \approx (2000, 2000)$. The coincidences in the tail part are due to the dissociation of metastable CO_2^{2+} and the formation of the $CO^+ + O^+$ pair in the drift region [15–20]. Thus, the relevant CO_2^{2+} states have lifetimes in the same order as the time-of-flight of CO_2^{2+} ($\sim$2 μs in the present case). The $C^+ + O^+$ structure also exhibits a diagonal feature, but the slope is steeper than -1. This feature in coincidences between fragments from the molecular center and one end is peculiar of two-step dissociation [21,22]: $CO_2^{2+} \rightarrow CO^+ + O^+ \rightarrow C^+ + O + O^+$. The feature of the $O^+ + O^+$ structure cannot be discussed, because a part of the structure is missing due to the detection dead time of 30 ns.

Auger electron spectra filtered by coincidences with $CO^+ + O^+$, $C^+ + O^+$, $O^+ + O^+$ and CO^{2+} are shown in Figures 2 and 3 for the C1s and O1s Auger decays, respectively. The intensities of the coincidence Auger spectra are corrected by assuming the 43% detection efficiency for each single ion, and thus the relative intensities of each band in the spectra directly reflect the branching ratio for the different fragmentation channels. Note that, because of the detection dead time, the intensity of the $O^+ + O^+$ spectrum should be underestimated.

One sees in Figures 2 and 3 that, while the total intensities of individual fragment channels are similar in the C1s and O1s Auger decays, the contributions from the individual dication states are

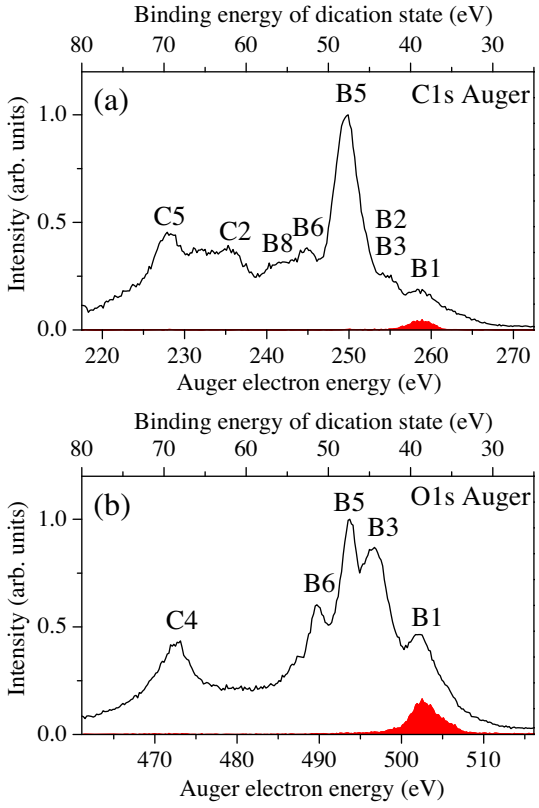

Figure 5. (a) C1s and (b) O1s Auger spectra (red) of CO_2 filtered by coincidences with metastable CO_2^{2+}, compared with total Auger spectra (black) which are the replots of the spectra in Figure 2a and b. (For interpretation of the references to color in this figure legend, the reader is referred to the web version of this article.)

largely different between the two Auger decays. The dication states in the binding energy range of 40–50 eV, which are the states with two outer-valence holes, are predominantly dissociate into the $CO^+ + O^+$ pair. This observation confirms the interpretations of the ion coincidence yields resulting from valence double photoionization [23] and from electron-impact double ionization [17]. A theoretical calculation proposed predissociation pathways of the dication states lying in this binding energy range into $CO^+ + O^+$ [24]. Figures 2 and 3 show that the dication states above 55 eV dissociate rarely into $CO^+ + O^+$ and preferably into the three-body fragmentation channels. The two-body fragmentation to $CO^{2+} + O$ is observed in a similar binding energy range to the three-body fragmentations, but the intensity is much weaker.

Next, we inspect the Auger final states relevant to metastable CO_2^{2+} and the mechanism of the site-specific formation. Auger electron spectra associated with the formation of metastable CO_2^{2+} can be extracted by filtering the coincidence events including a single ion signal in the time-of-flight range of 2000–2060 ns (see Figure 4a). The coincidence Auger electron spectra thus obtained are plotted in Figure 5, in comparisons with the total Auger spectra. One finds in both coincidence spectra that the formation of metastable CO_2^{2+} is associated with only the lowest band (B1) attributed to the $1\pi_g^{-2}$ configuration. The main contributors to this band are calculated to be the $a^1\Delta_g$ and $b^1\Sigma_g^+$ states of the $1\pi_g^{-2}$ configuration [12,14], while a high-resolution C1s Auger spectrum shows a certain contribution from the $c^1\Sigma_u^-$ state in this band [11]. The potential energy surfaces of these CO_2^{2+} states are calculated to have deep minima [24,25], and in practice these CO_2^{2+} states populated by valence double photoionization are observed to have lifetimes in the order of μs or more [15].

The intensities of the B1 structures in the coincidence spectra do not reproduce the whole intensities in the corresponding ranges of the total Auger spectra, and other components underlie the B1 structures in the total spectra. Apart from background signals, the Auger decay of the photoionization satellite states, which preferably produces excited CO_2^{2+} states by spectator behavior of initially-excited electrons, should contributes to the yields in this energy range. The Auger electron spectra filtered by coincidences with $C^+ + O^+$, shown in Figures 2c and 3c, exhibit some intensities in this energy range, which is probably due to the dissociation of the excited CO_2^{2+} states produced by the Auger decay of the photoionization satellite states.

In Figure 5, while the CO_2^{2+} states in the same binding energy range are relevant to the metastable CO_2^{2+} formation following the different core–hole creations, the intensity of the metastable CO_2^{2+} formation in the O1s core–hole decay is much higher than that in the C1s one, as already observed in the time-of-flight spectra in Figure 1. The favorable production of the relevant $1\pi_g^{-2}$ states following the O1s core–hole creation is qualitatively explained by considering the charge distribution of the $1\pi_g$ orbital involved in the Auger decay processes. Since the $1\pi_g$ orbital with the dominant oxygen lone-pair character is largely localized around the O atom in the CO_2 molecule, the O1s core–hole is filled preferentially by the $1\pi_g$ electron [11]. Thus the Auger transition involving the $1\pi_g$ electrons is favored in the decay of the O1s core–hole states, resulting in the favorable formation of metastable CO_2^{2+} states with the configuration of $1\pi_g^{-2}$.

In conclusion, the mechanism of the site-specific formation of metastable CO_2^{2+} following inner-shell ionization of CO_2 has been studied by using an Auger-electron–ion coincidence method. The site-specificity arises from the two conditions: (1) only dication states of $1\pi_g^{-2}$ are relevant to the metastable formation, and (2) the formation of these dication states are favorable in the O1s Auger decay, because of the charge distribution of the $1\pi_g$ orbital localized at the O site. Such conditions may be often fulfilled for the Auger decay in which valence electrons with localized and non-bonding characters are involved, and thus site-specific formation of metastable dication may occur in many other molecules.

Acknowledgements

The authors are grateful to the staff of the UVSOR facility for their support and stable operation of the storage ring during the course of the present experiment. This work was supported by the Cooperative Research Program of the Institute for Molecular Science.

References

[1] W. Eberhardt, T.K. Sham, R. Carr, S. Krummacher, M. Strongin, S.L. Weng, D. Wesner, Phys. Rev. Lett. 50 (1983) 1038.
[2] I. Nenner, P. Morin, U. Becker, D.A. Shirley (Eds.), VUV and Soft X-ray Photoionization Studies in Atoms and Molecules, Plenum Press, London, 1996 (And references therein).
[3] C. Miron, M. Simon, N. Leclercq, D.L. Hansen, P. Morin, Phys. Rev. Lett. 81 (1998) 4104.
[4] S. Wada, H. Kizaki, Y. Matsumoto, R. Sumii, K. Tanaka, J. Phys. Condens. Matter 18 (2006) S1629.
[5] G. Ohrwal et al., J. Phys. B 35 (2002) 4543.
[6] T. Kaneyasu, Y. Hikosaka, E. Shigemasa, AIP Conf. Proc. 879 (2007) 1793.
[7] T. Kaneyasu, Y. Hikosaka, E. Shigemasa, J. Electron Spectrosc. Relat. Phenom. 156–158 (2007) 279.
[8] D. Céolin, C. Mirona, M. Simona, P. Morin, J. Electron Spectrosc. Relat. Phenom. 141 (2004) 171.
[9] W.E. Moddeman, T.A. Carlson, M.O. Krause, B.P. Pullen, W.E. Bull, G.K. Schweitzer, J. Chem. Phys. 55 (1971) 2317.
[10] A. Hiltunen, S. Aksela, Gy Víkor, S. Ricz, Á. Kövér, B. Sulik, Nucl. Instrum. Meth. Phys. Res. B 154 (1999) 267.
[11] R. Püttner et al., J. Phys. B At. Mol. Opt. Phys. 41 (2008) 045103.
[12] J.A. Kelber, D.R. Jennison, R.R. Rye, J. Chem. Phys. 75 (1981) 652.
[13] J.H.D. Eland et al., J. Chem. Phys. 135 (2011) 134309.
[14] H. Ågren, J. Chem. Phys. 75 (1981) 1267.
[15] A.E. Slattery et al., J. Chem. Phys. 122 (2005) 084317.

[16] V. Sharma, B. Bapat, J. Mondal, M. Hochlaf, K. Giri, N. Sathyamurthy, J. Phys. Chem. A 111 (2007) 10205.
[17] S.J. King, S.D. Price, Int. J. Mass Spectrom. 272 (2008) 154.
[18] M. Alagia et al., J. Phys. Chem. A 113 (2009) 14755.
[19] M. Alagia et al., Phys. Chem. Chem. Phys. 12 (2010) 5389.
[20] M. Alagia et al., Chem. Phys. 398 (2012) 134.
[21] J.H.D. Eland, Mol. Phys. 61 (1987) 725.
[22] C. Tian, C.R. Vidal, Phys. Rev. A 58 (1998) 3783.
[23] T. Masuoka, Phys. Rev. A 50 (1994) 3886.
[24] D. Zhang, B. Chen, M. Huang, Q. Meng, Z. Tian, J. Chem. Phys. 139 (2013) 174305.
[25] M. Hochlaf, F.R. Bennett, G. Chambaud, P. Rosmus, J. Phys. B: At. Mol. Opt. Phys. 31 (1998) 2163.